iScience

CellPress
OPEN ACCESS

Article

Reshaping tumor immune microenvironment by Epstein-Barr virus activation in the stroma of colorectal cancer

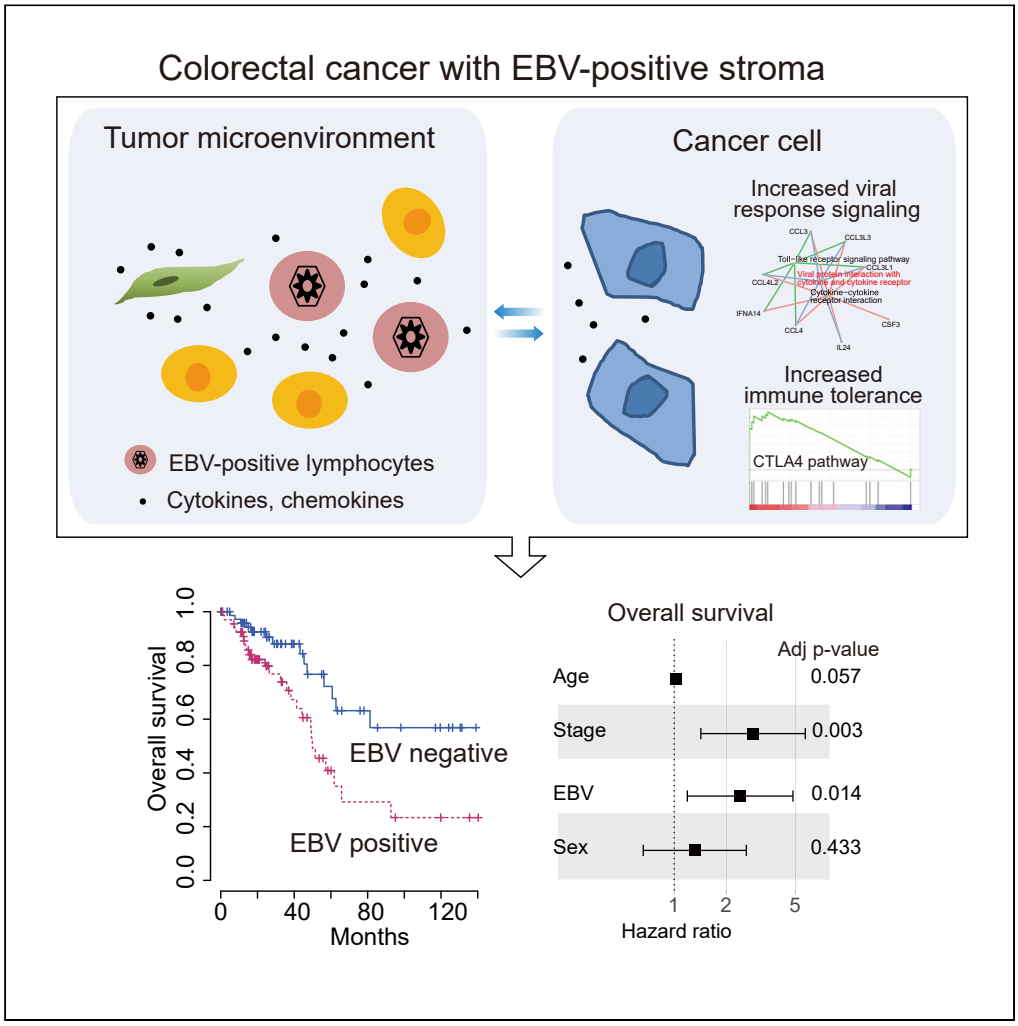

Hyun Ju Park, Eun Jeong Cho, Ji-Hun Kim, Sehun Lim, Chang Ohk Sung

anespc@naver.com (S.L.)
co.sung@amc.seoul.kr (C.O.S.)

Highlights

EBV expression was identified in tumor stroma of CRC

CRC with the EBV-positive stroma has different immune composition and poor prognosis

Immune tolerance signaling in cancer cells against EBV are enriched

Park et al., iScience 26, 105919
January 20, 2023
https://doi.org/10.1016/j.isci.2022.105919

iScience

CellPress
OPEN ACCESS

Article

Reshaping tumor immune microenvironment by Epstein-Barr virus activation in the stroma of colorectal cancer

Hyun Ju Park,[1] Eun Jeong Cho,[2] Ji-Hun Kim,[1] Sehun Lim,[3,*] and Chang Ohk Sung[1,2,4,*]

SUMMARY

The formation of tumor immune microenvironment (TIM) is complicated and poorly understood. Little is known about the effect of a viral infection potentially inducing an additional immune response in the TIM. Here, we identify Epstein-Barr virus (EBV) expression in the TIM in colorectal cancer (CRC) tissue through EBV-encoded RNA *in-situ* hybridization and RNA sequencing data and investigate the effects of EBV on TIM composition and clinical outcomes. EBV was detected in tumor-infiltrating lymphocytes, but not in cancer cells. EBV positivity was associated with older age, male sex, and *SMAD4* mutations. EBV-positive tumors were characterized by enrichment in chemokine/cytokine signaling pathways and altered immune cell composition, including plasma and CD4 T cells, as well as cancer cells intrinsically enriched pathways related to immune tolerance, leading to poor prognosis. In conclusion, we identified EBV expression in TIM and suggested its association with poor prognosis by altering the TIM in CRC.

INTRODUCTION

The formation of the tumor microenvironment (TIM) is affected by various factors. As cancer cells interact closely with stromal cells and immune cells,[1] the signals from cancer cells are known to be one of the major factors in forming the TIM. T cell depletion in TIM can be induced by WNT/ß-catenin signaling from cancer cells.[2] Microsatellite instability-high (MSI-H) tumors characterized by hypermutation show abundant immune cell infiltration, which is beneficial for immunotherapy.[3] In addition, various signaling caused by oncogenic mutations, including *KRAS* and *TP53* are known to characterize the TIM.[4] However, other than these cancer cell-related signals, at present, limited information is available on the factors related to patient characteristics.

Epstein-Barr virus (EBV) infection increases the risk of several malignant tumors, including nasopharyngeal carcinoma, malignant lymphoma, and gastric cancer.[5] However, the effect of the EBV expression in lymphocytes at tumor stroma, and ultimately the effect on TIM composition of TIM changes, is little known in colorectal cancer (CRC). Recently, we identified that EBV was activated in tumor-infiltrating B lymphocytes in a subset of hepatocellular carcinoma (HCC) with abundant immune cell infiltrate.[2] HCCs with EBV activation in the TIM have a poor prognosis despite abundant immune cell infiltration in the tumor. This suggests that some infiltrating immune cells do not attack cancer cells but may be related to the chemotaxis of immune cells based on the activity of EBV. Specific organs, such as the liver, do not have direct contact with the external environment, and typically do not have immune cells in their tissues. However, hollow viscous organs, such as the intestine, have resident immune cells for protection from external pathogens. However, the effect of EBV expression in TIM on the composition of TIM or the prognosis of patients with malignant diseases in these hollow viscous organs is not known.

Therefore, we investigated the presence of EBV expression in the CRC microenvironment and the effect of EBV expression on the immune cell composition of the TIM and its clinical significance in CRC.

RESULTS

EBV expression in tumor-infiltrating lymphocytes in colorectal cancer

First, we evaluated EBV in 87 CRC tissues and identified EBV in TILs in the CRC tissues using EBV-ISH to detect EBV-encoded RNA, which is the gold standard for detecting latent EBV (Figure 1A). Of the total

[1]Department of Pathology, Asan Medical Center, University of Ulsan College of Medicine, 88 Olympic-ro 43-gil, Songpa-gu, Seoul, Republic of Korea

[2]Department of Medical Science, Asan Medical Institute of Convergence Science and Technology, Asan Medical Center, University of Ulsan College of Medicine, Seoul, Republic of Korea

[3]Department of Anesthesiology and Pain Medicine, Busan Paik Hospital, Inje University College of Medicine, Busan 47392, Republic of Korea

[4]Lead contact

*Correspondence: anespc@naver.com (S.L.), co.sung@amc.seoul.kr (C.O.S.)

https://doi.org/10.1016/j.isci.2022.105919

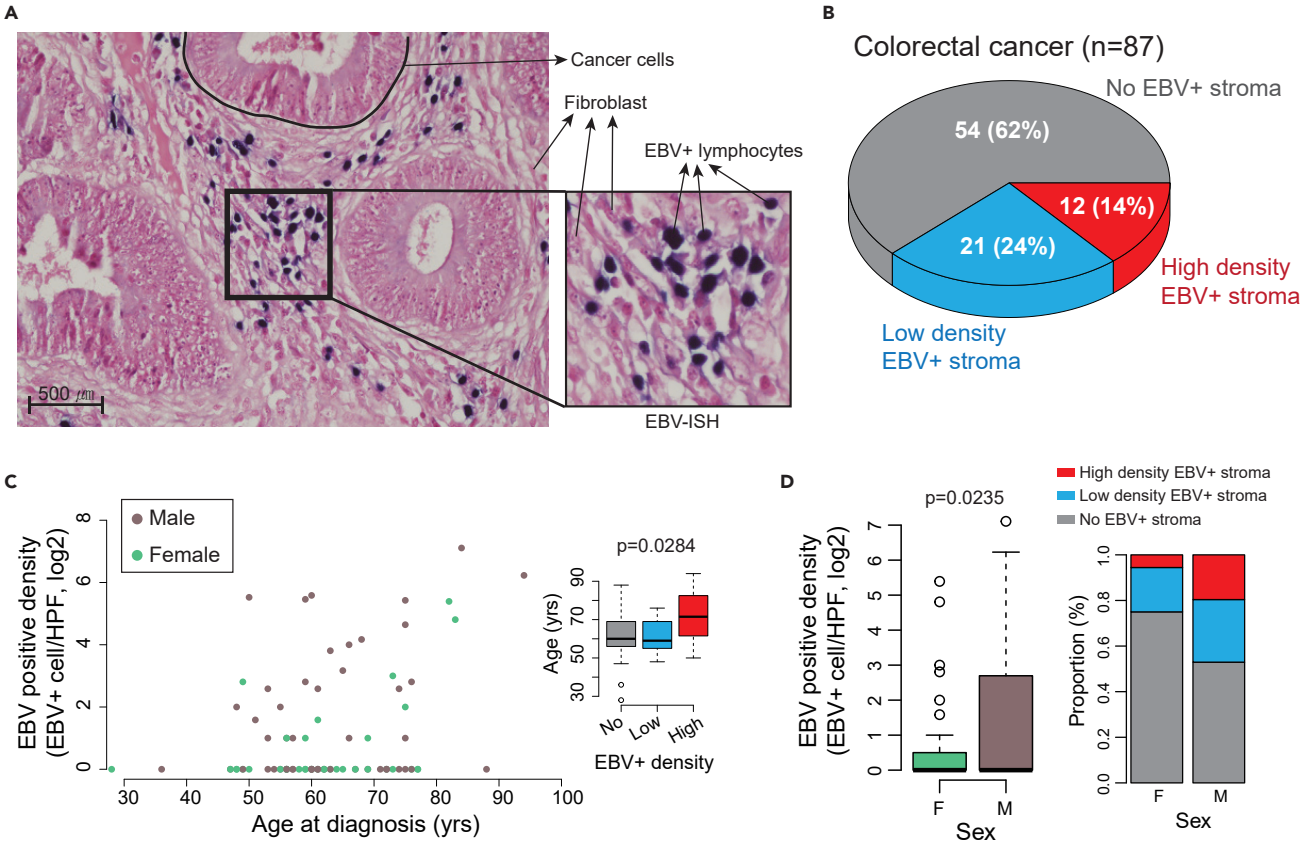

Figure 1. Epstein-Barr virus (EBV) activation in tumor stroma

(A) *In situ* hybridization (ISH) to Epstein-Barr virus (EBV)-encoded RNA (EBER) for detecting and localizing latent EBV (bar = 500 μm). EBVs were positive for tumor infiltrating lymphocytes.

(B) EBVs were positive in 38% of cancer tissue.

(C) EBV positivity, specifically in high EBV positivity, was increased with age (Kruskal-Wallis test).

(D) EBV positivity was identified more frequently in males (Wilcoxon rank sum test).

87 CRC samples, 38% showed EBV positivity in TILs; 12 (14%) showed high EBV-positive density (>10 cells/HPF), and 21 (24%) showed low EBV-positive density (Figure 1B). EBV expression was not detected in cancer cells in all 87 CRC samples. EBV-positivity was significantly associated with older age at diagnosis ($p = 0.0284$, Figure 1C) and male patients ($p = 0.0235$, Figure 2D).

Clinical significance of EBV positivity in tumor microenvironment

The presence of the EBV viral genome was investigated in RNA-seq data, which indicates EBV gene expression. In addition, to determine whether EBV detection in RNA-seq data could represent EBV-ISH results in tissues, we compared results from cancer tissue and corresponding cancer cell organoid RNA-seq data with EBV-ISH results. We found that EBV-ISH results in cancer tissues significantly correlated with EBV positivity detected in RNA-seq data ($p = 1.19e-05$), whereas in cancer organoids composed of only cancer cells, EBV positivity was not correlated with EBV-ISH (Figure 2A), which indicates that the primary source of EBV positivity in CRC is TIM. In particular, high-density EBV positivity in EBV-ISH had a good correlation with RNA-seq results (Figure 2B, left), and these patients tended to have a poor prognosis (Figure 2B, right).

Because we found the correlation in EBV positivity between EBER-ISH and RNA-seq in cancer tissues, we collected RNA-seq data from the TCGA CRC to overcome the small size of our AMC cohort. The EBV viral genome was examined from a total of 292 TCGA CRC RNA-seq data generated using the Illumina Hi-Seq platform (Figure 2C). EBV viral sequence was detected in 53% of the TCGA CRC. The EBV-positivity was also significantly associated with older age (Figure 2D). In addition, in this large independent cohort, EBV-positivity was significantly associated with poor prognosis in both overall ($p = 0.021$) and

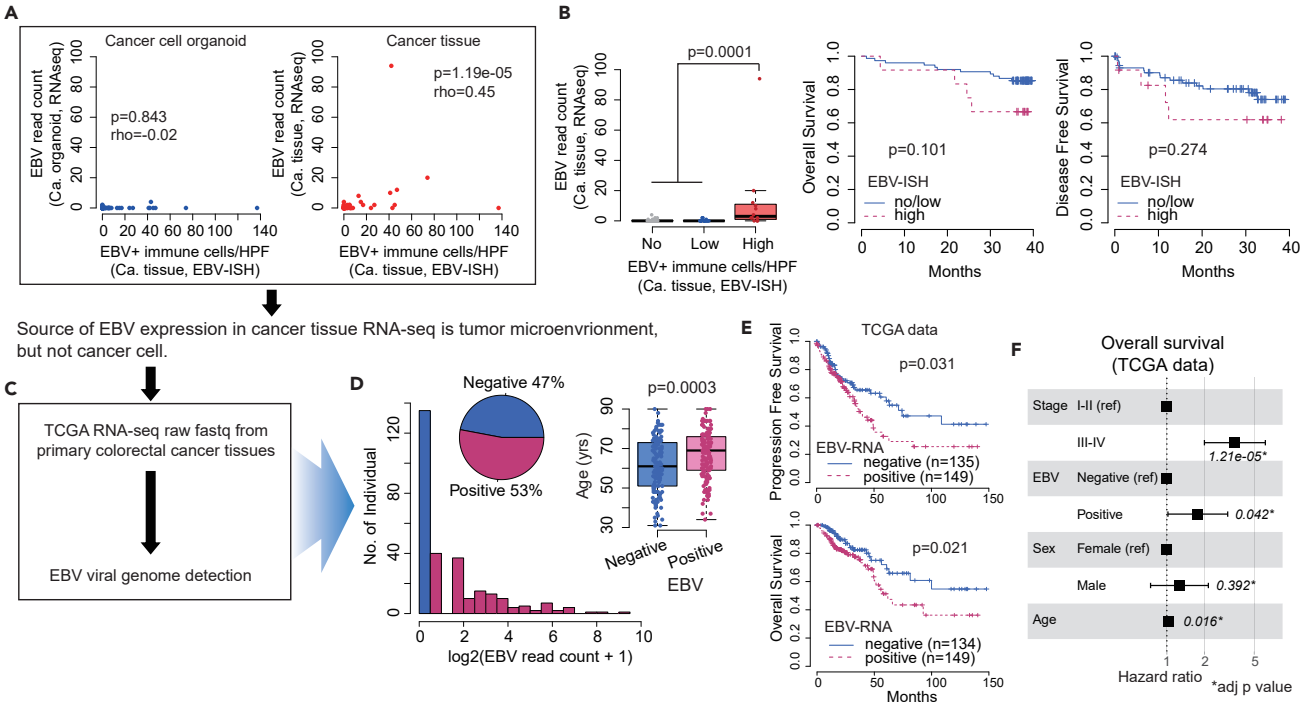

Figure 2. Epstein-Barr virus (EBV) detected in RNA-seq

(A) EBV viral genome was not detected in organoids (cancer cells only); however, it was frequently detected in cancer tissue, which was correlated with detection by EBV-ISH in cancer tissue.

(B) High EBV positivity by EBV-ISH showed high EBV sequence read counts in tissue RNA-seq (Wilcoxon rank sum test), and the patients with high EBV positivity had a tendency for poor prognosis.

(C) Because EBV from tissue RNA-seq correlated with EBV-ISH, EBV viral reads were detected from a large RNA-seq dataset of colorectal cancer from TCGA.

(D) EBV was detected in half of TCGA colorectal cancer tissues, and positivity was also associated with increased age (Wilcoxon rank sum test).

(E) Survival analysis revealed a significantly poor prognosis in patients with EBV positive (log-rank test).

(F) EBV positivity was an independent prognostic factor after adjustment for stage, age, and sex (Multi-variated Cox regression test).

progression-free survival (p = 0.031) (Figure 2E). Because EBV-positivity was associated with sex and age of the patients, these confounding factors and tumor stage were adjusted, and the EBV-positivity was still significantly associated with poor prognosis (Figure 2F).

Characteristics of EBV-positive tumor immune microenvironment

Tumor-infiltrating immune cells were profiled from RNA-seq normalized gene expression data of TCGA CRC and compared with EBV-positivity (Figure 3A). When EBV infects, it releases its antigen, consequently triggering immune response naturally and recruiting a variety of immune cells.[6] Total amount of immune cells between the EBV-positive group and negative group did not differ (Figure 3B); however, the composition (Figure 3C) and absolute amount (Figure 3D) of immune cells, including plasma cell, CD4 T cell, NK cell, and myeloid dendritic cell were significantly different between EBV-positive tumor stroma and EBV-negative tumor stroma in CRC. Among these immune cell types, plasma and CD4 T cells and the age of the patients were independently associated with EBV-positivity (Figure 3E). In terms of signaling pathways, it was confirmed that B cell and T cell receptor signaling pathways were enriched in the EBV-positive group (Figure 3F).

Next, to investigate the reason for poor prognosis despite enriched immune cell signaling, we first assessed the presence or absence of T cell exhaustion. As expected, T cell exhaustion was associated with a high tumor mutation burden (p = 1.32e-07, Figure 3F), but not with EBV positivity (Figure 3H), which was different from the results in our previous study in HCC.[2] We speculated that this might be due to the characteristics of hollow viscous organs, which have continuous contact with outside pathogens and contain resident immune cells. However, we identified that the immunodeficiency signaling was relatively enriched in the EBV-positive group in both data sets (Figure 3I).

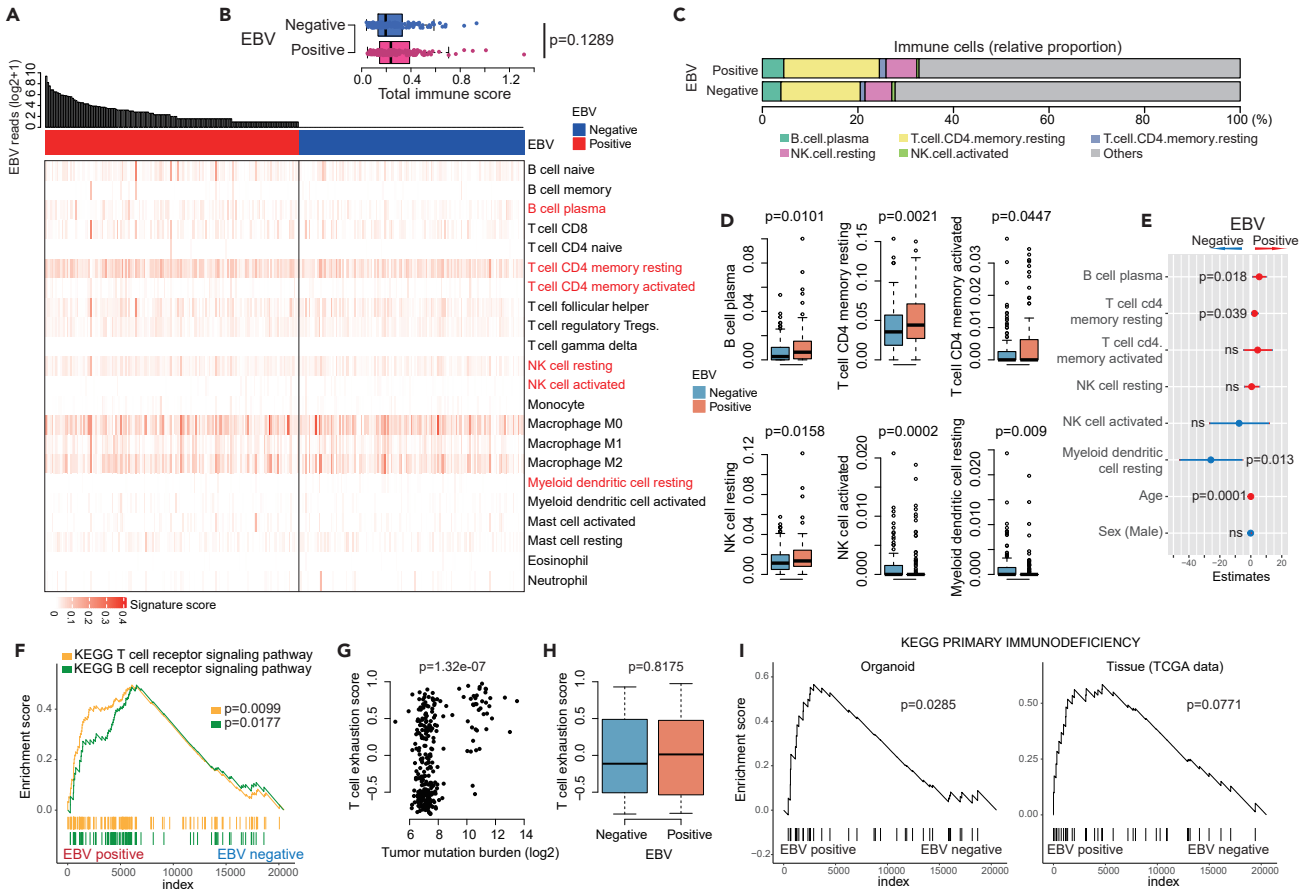

Figure 3. Tumor immune microenvironment of colorectal cancer with EBV-positive stroma

(A) Immune cell profiling and quantification using CIBERSORT in primary cancer tissue (TCGA data) and EBV-positivity.

(B) Total immune score between EBV-positive and EBV-negative tumor (Wilcoxon rank sum test).

(C) Different composition of infiltrating immune cell types in EBV-positivity.

(D) Major changes in different immune cell types included an increase in plasma cells, CD4 T cells, and resting NK cells in EBV-positive cancer, whereas activated NK cells and resting myeloid dendritic cells decreased (Wilcoxon rank sum test).

(E) Immune cell types and clinical factors associated with EBV-positivity using TCGA CRC data (multivariate logistic regression analysis).

(F) Pathway analysis showed enriched T cell and B cell receptor signaling in EBV-positive cancer tissue (GSEA analysis using KEGG database).

(G and H) T cell exhaustion was associated with a high tumor mutation burden; however, it was not associated with EBV-positivity in colorectal cancer (Wilcoxon rank sum test).

(I) However, tissue with EBV-positivity tended to have immunodeficiency status (GSEA analysis using KEGG database).

Cancer signaling associated with EBV-positivity

Somatic mutations were compared between the EBV-positive group and the EBV-negative group (Figure 4A). Among the various somatic mutations, *SMAD4* mutations tended to be increased in the EBV-positive group in the combined TCGA and AMC data set (p = 0.016, Figure 4B). In addition, various cancer-associated oncogenic signaling pathways were enriched in the EBV-positive group, which may contribute to cancer cell proliferation related to poor prognosis (Figure 4C).

Distinct prognostic effect of EBV-positivity in immune-cold tumor

TCGA CRC was divided into two groups, immune-inflamed (“immune-hot”) tumors and immune-desert (“immune-cold”) tumors based on the median of the total immune score (sum of each immune cell score) (Figure 5A). First, to validate this classification, the association between TMB and the classification of tumor based on the total immune score was examined. Consistent with other studies,[7,8] immune-hot tumors showed high TMB (p = 0.0079, Figure 5B). Then, the prognostic effect of EBV positivity in each tumor group was investigated. Of interest, EBV positivity had no effect on prognosis in immune-hot tumors (Figure 5C), but was significantly associated with a worse prognosis for progression-free survival (p = 0.045) and overall

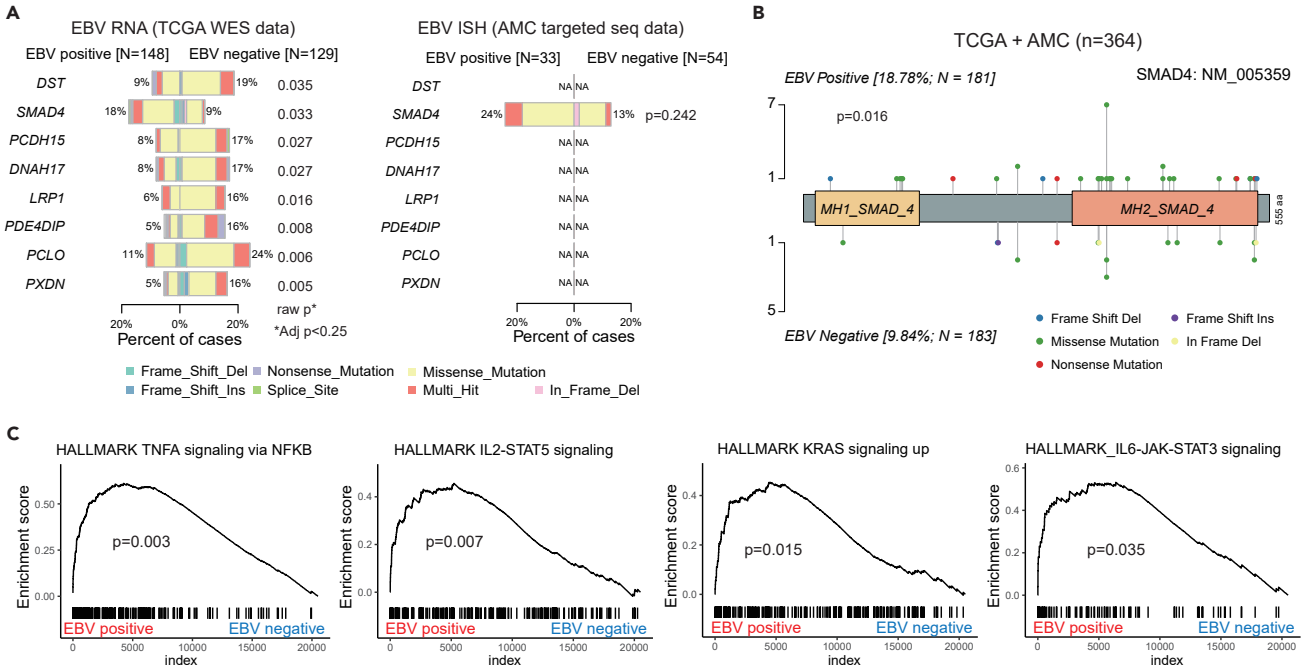

Figure 4. Cancer signaling in colorectal cancer with EBV-positivity

(A) Somatic mutation analysis revealed an increased tendency of SMAD4 mutation in colorectal cancer with EBV-positivity (Fisher exact test).

(B) Lollipop plot of SMAD4 mutation.

(C) Cancer pathways, including TNFA signaling, were enriched in colorectal cancer with EBV-positive GSEA analysis using the Cancer Hallmark gene set.

survival (p = 0.004) in immune-cold tumors (Figure 5D). The significance of the prognostic effect of EBV-positivity in the immune-cold tumor was maintained even after adjustment for tumor stage, sex, and age (Figure 5E).

Different TIM of EBV positivity in immune-cold tumor

After obtaining differentially expressed genes (DEGs) between EBV-positive and EBV-negative groups in immune-cold tumors from the TCGA data set, the functions of these DEGs were investigated using gene ontology analysis. Genes related to collagen were reasonably enriched in EBV-negative immune-cold tumors (Figure 6A). However, some immune-related signaling pathways including viral protein interaction with cytokines and cytokine receptors were enriched in EBV-positive immune-cold tumors compared to EBV-negative immune-cold tumors (Figure 6B). The enriched pathways and related gene networks in EBV-negative immune-cold tumors are shown in Figure 6C. As a representative example, *COL1A1*, which encodes parts of type I collagen, was highly expressed in EBV-negative immune-cold tumors, and the histology of corresponding tumor also showed increased fibrosis (Figure 6D). Despite tumor immune type, infiltrating immune cells were observed histologically in EBV-positive tumors with low *COL1A1* expression (Figure 6E). In EBV-positive immune-cold tumor, the various signaling pathways related to tumor immune were also enriched (Figure 6F), similar to the results in Figure 4C. Of interest, inflammatory cancer-associated fibroblast (iCAF) signature, which is well known to be associated with poor prognosis in cancer, was significantly increased in EBV-positive compared to that in the EBV-negative immune-cold tumors (Figure 6G).

Inferred hypothesis for poor prognosis of EBV positivity in immune-cold tumor

To reveal whether EBV positivity in TIM was related to changes in gene expression in cancer cells, we further analyzed colorectal cancer organoid genomic data in immune-cold tumors. We identified cancer-intrinsic gene expressions (organoid data) significantly correlated with the increased EBV-ISH positivity in TIM (cancer tissue data). These genes were significantly associated with viral protein interaction with cytokines and cytokine receptor pathways (Figure 7A). Total immune scores indicating that the total amount of tumor-infiltrating immune cells did not differ between EBV-positive and EBV-negative immune-cold tumors in two independent data sets (Figure 7B). Pathway analysis showed that cancer cells intrinsically enriched

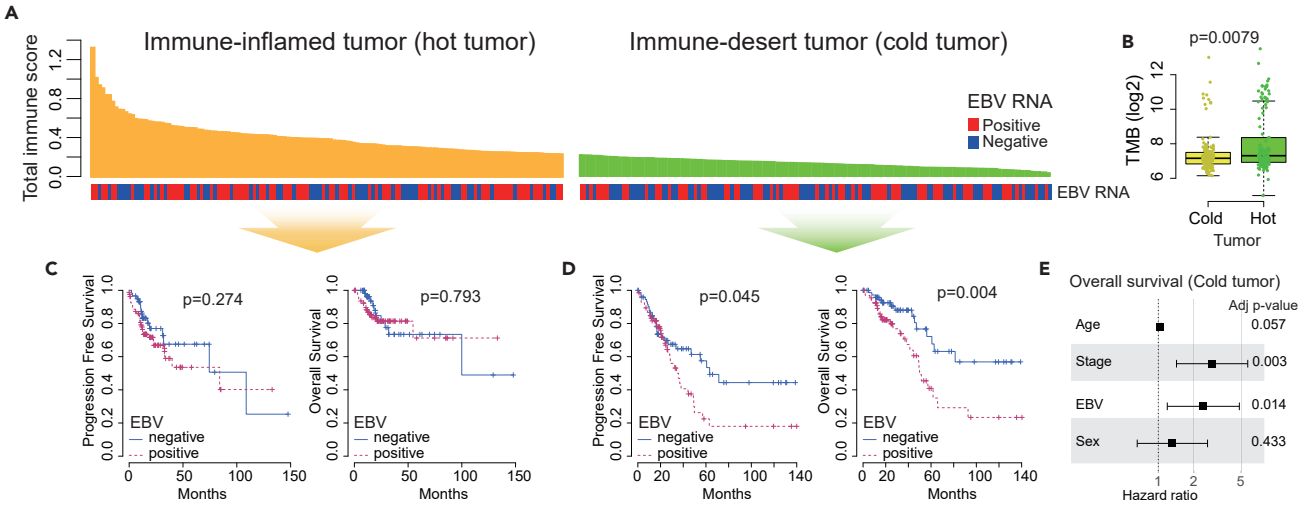

Figure 5. Prognostic impact of EBV positivity in immune-cold tumors

(A) Colorectal cancers (TCGA data) were divided into two groups by the median value of the total immune score.

(B) Immunologically hot tumors were associated with high tumor mutation burden (Wilcoxon rank sum test).

(C) No prognostic effect of EBV positivity was observed in immune-hot tumors (log-rank test).

(D and E) However, EBV had a strong prognostic effect in immune-cold tumors (log-rank test) and was also an independent prognostic factor (Multivariated Cox regression test; data are represented as hazard ratio +/− 95% confidence interval).

pathways related to immune tolerance, such as the CTLA4 pathway (Figure 7C). Collectively, in the immune-cold tumors, low levels of immune cell infiltration may be mainly related to EBV, and various viral-related chemokine and cytokine signaling with increased immune tolerance of cancer cells may contribute their progression (Figure 7D).

DISCUSSION

We have identified EBV expression in TILs of a subset of CRC. EBV was positive at significantly higher frequencies in males and the elderly. Because EBV is in the latent phase in most populations,[9] this might result from an age-related decline of immune function,[10] which can cause the re-activation of the EBV virus. It is also possible that the TIM changed by the cancer cells created an environment favorable for EBV expression. Indeed, in this study, the EBV positivity was higher in CRC with *SMAD4* mutation. Therefore, we think that the formation of TIM can be complicated by the effect of cancer cells and EBV expression in TIL.

In EBV infection, CD8 T cells, CD4 T cells, and NK cells are one of the main responder immune cells.[6] In this study, increased CD4 T cells in the EBV-positive CRC have been found. However, a lack of difference in CD8 T cells may be because of persistent EBV infection[6] and the microenvironment changes caused by cancer cells.

We confirmed that EBV expression in TILs in CRC reshapes the TIM and is associated with poor prognosis, as in our previous study using HCC.[2] This similar finding strongly suggests that EBV expression in TIM affects the behavior of tumors. In HCC, EBV positivity in TIM showed severe immune cell infiltration,[2] however, in CRC, no significant difference in the total amount of immune cell infiltration was found. In HCC, the EBV-ISH testing showed EBV positivity in less than 5% of HCCs,[2] but in CRC, it was positive in approximately 30%. These differences are probably because of the characteristics of the primary organ between solid and hollow viscous organs.

However, despite relatively increased immunogenic signals, including viral protein interaction with cytokines and cytokine receptors in tumors with EBV expression in TIM, the association with poor prognosis suggests that the qualitative characteristics of immune cells in TIM are important for clinical prognosis. This context may also indicate that EBV expression in TIM may affect the immunotherapy response.

In this study, the mechanism of EBV reshaping the TIM was not revealed because of the unavailability of a suitable animal model. We were not able to suggest a mechanism based on a specific causal relationship;

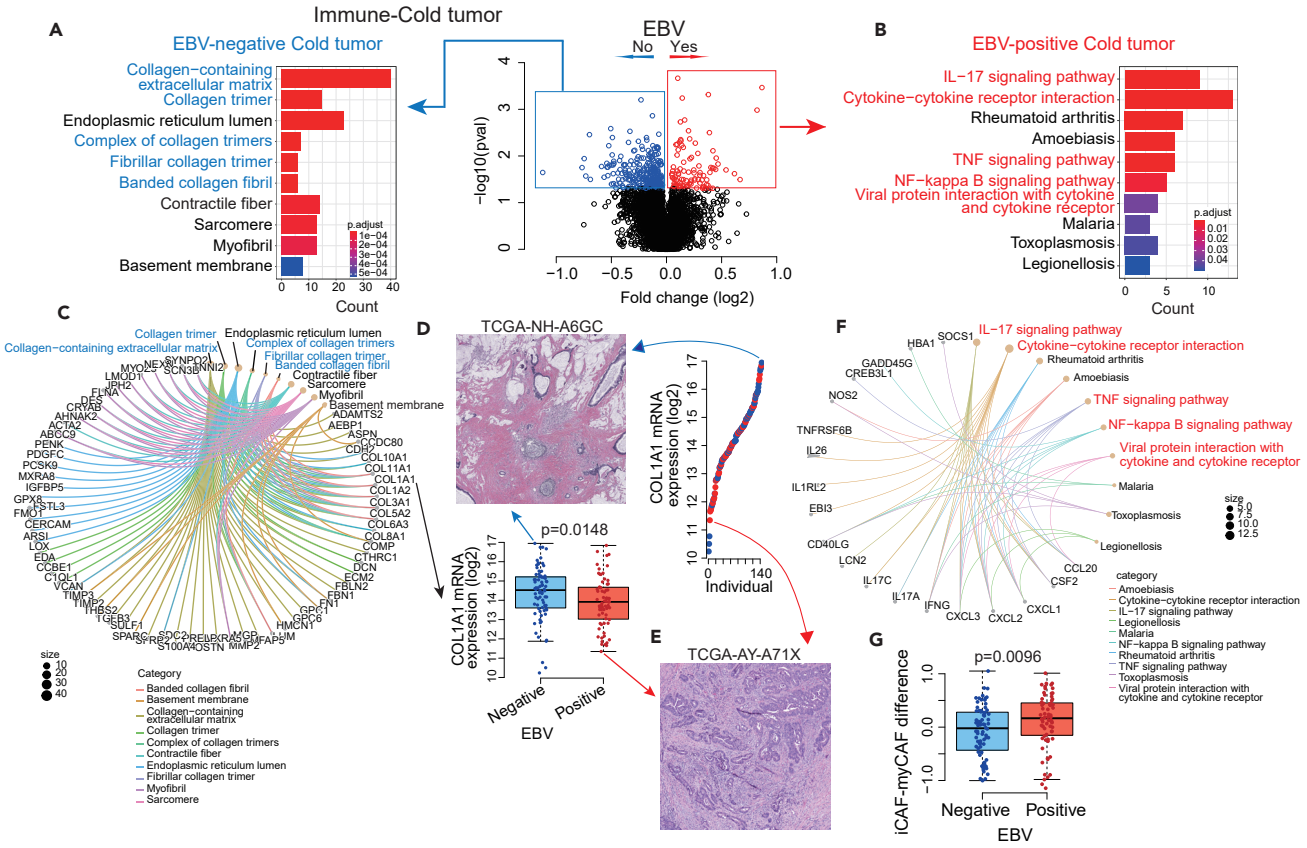

Figure 6. Tumor immune microenvironment according to EBV positivity in immune-cold CRC

(A and B) Differentially expressed genes and pathways between EBV positive and EBV negative immune-cold tumor.

(C) Fibrosis-related gene signatures were enriched in EBV-positive immune-cold tumor.

(D and E) For example, higher *COL1A1* gene expression was present in EBV-negative immune-cold tumors (Wilcoxon rank sum test). Hematoxylin-eosin stained image showed increased collagen (fibrosis) deposition in EBV-negative immune-cold tumors with the highest *COL1A1* expression, whereas scattered immune cell infiltrations were present in EBV-positive immune-cold tumor with the lowest *COL1A* expression.

(F) Inflammatory pathway signatures, including viral protein interaction with cytokines and cytokine receptors, were enriched in EBV-positive immune-cold tumors compared to those of EBV-negative immune-cold tumors.

(G) Relative iCAF signature adjusted by myCAF signature was elevated in EBV-positive immune-cold tumor (Wilcoxon rank sum test).

however, using two independent datasets of the TCGA and AMC cohorts, we were able to conclude that the characteristics of the TIM were different in patients with EBV-positive colorectal cancer compared to those in the EBV-negative group. As the inflammatory pathways mainly related to viral infection (viral protein interaction cytokine and cytokine receptor pathway) were significantly enriched, we speculate that different types of immune cells may be mobilized according to these signals, and the composition of TIM may change accordingly.

We did not show direct evidence for the causal relationship between TIM EBV-positivity and cancer cell progression. Therefore, it will be important to reproduce the tumor progression using animal models with EBV-positive TMI. However, the technology for creating animal models related to EBV is mainly focused on creating models for EBV-associated lymphoproliferative disease or host immune response to EBV infection.[11,12] Therefore, generating an animal model for cancer cells with EBV-positive tumor stroma will be valuable to understand the mechanism of the causal relationship.

It is well known that EBV infection in the epithelial cells or immune cells gives rise to carcinoma or hematologic malignancies. However, besides the direct development of tumors by EBV, little is known about EBV being expressed in lymphocytes of the TIM, changing the composition of the TIM and cancer cell-intrinsic signature, and thus affecting the behavior of the tumor. Therefore, this study confirmed that

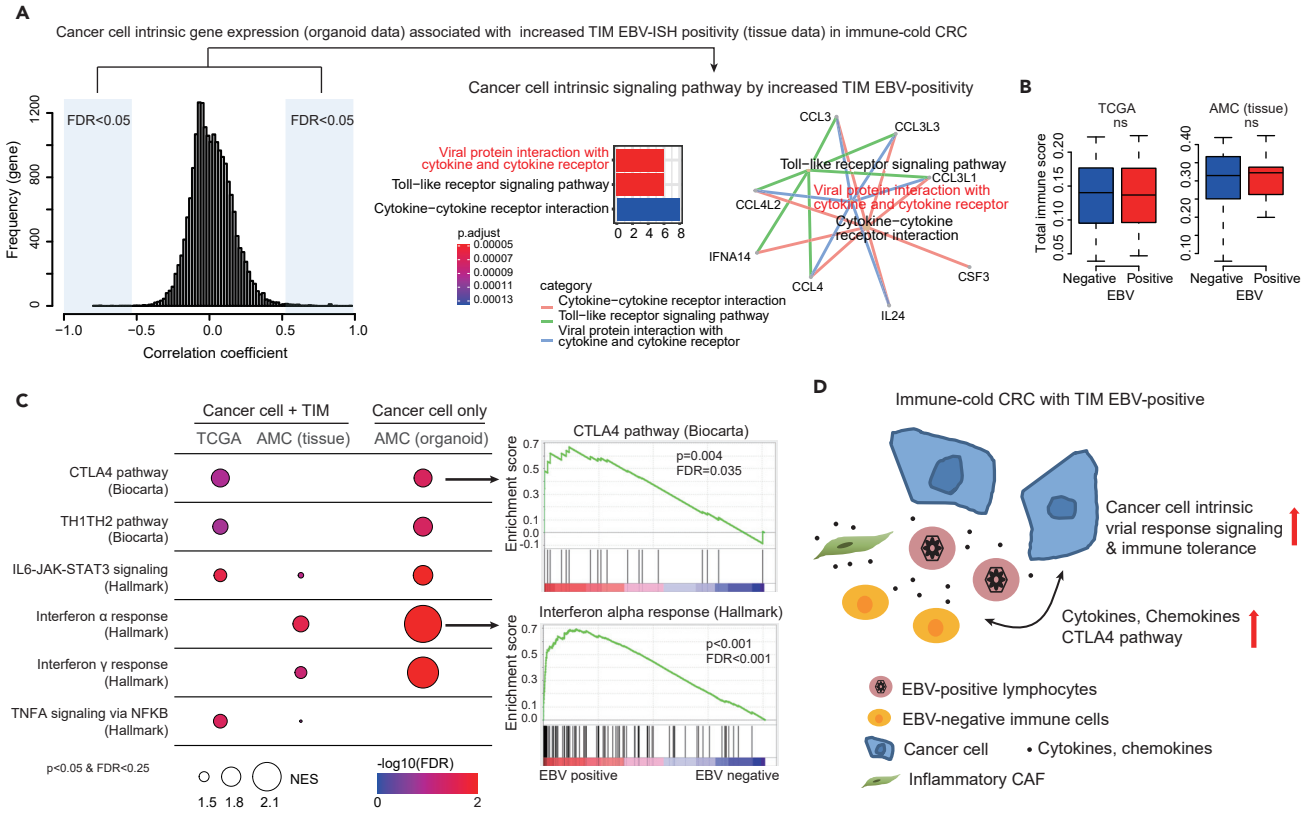

Figure 7. Inference for poor prognosis of EBV-positivity in immune-cold tumor

(A) Cancer cell intrinsic gene expressions associated with increased EBV-ISH positivity in TIM using cancer cell organoids and matched cancer tissue (FDR from Pearson correlation test).

(B) No significant differences in total immune score between EBV-positive and EBV-negative in both TCGA and AMC cohorts were found (Wilcoxon rank sum test).

(C) Enriched pathways in cancer tissue and cancer cell from immune-cold CRC with EBV-positive stroma compared to those from immune-cold CRC with EBV-negative stroma (GSEA analysis).

(D) EBV activity induced viral-associated immune response and released various cytokines, which also affected cancer cell-intrinsic signatures, including the upregulated CTLA4 pathway and may contribute to cancer progression.

EBV expression in tumor-infiltrating lymphocytes according to the characteristics of patients, such as age, affects the TIM as well as cancer cells.

Limitations of the study

We showed that the composition of TIM was different according to the EBV positivity using two independent datasets of TCGA and AMC cohorts as the inflammatory pathways mainly related to viral infection were significantly enriched. We also showed the relationship between EBV expression and poor prognosis in CRC by increased chemokine/cytokine signaling pathways and cancer cells intrinsically enriched pathways related to immune tolerance. However, a direct evidence and mechanism based on a specific causal relationship between TIM EBV-positivity and cancer cell progression was not clarified owing to the unavailability of a suitable animal model that can artificially regulate EBV expression in B cells in the TIM of CRC. Therefore, generating an animal model for cancer cells with EBV-positive tumor stroma will be valuable in a future study.

STAR★METHODS

Detailed methods are provided in the online version of this paper and include the following:

- KEY RESOURCES TABLE
- RESOURCE AVAILABILITY

ACKNOWLEDGMENT

This study was supported by the Basic Science Research Program through the National Research Foundation of Korea (NRF), funded by the Ministry of Science, ICT & Future Planning (NRF-2019R1A2C1084460), a grant of the Korea Health Technology R&D Project through the Korea Health Industry Development Institute (KHIDI), funded by the Ministry of Health & Welfare, Republic of Korea (grant number: HR21C0198), the Bio & Medical Technology Development Program of the National Research Foundation (NRF) funded by the Korean government(MSIT) (No. NRF-2022M3E5F3081268), and a grant from Research year of Inje University in 2012 (20121030).

AUTHOR CONTRIBUTIONS

C.O.S. designed and conceptualized the study. C.O.S., E.J.C., and H.J.P. analyzed the data and interpreted the results. J.H.K. contributed materials and interpretation. C.O.S., H.J.P., and E.J.C. wrote the manuscript. S.L. reviewed the manuscript. All authors read and approved the final manuscript.

DECLARATION OF INTERESTS

The authors declare that they have no competing interests.

Received: September 9, 2022
Revised: November 28, 2022
Accepted: December 29, 2022
Published: January 20, 2023

REFERENCES

1. Lee, K.W., Yeo, S.Y., Gong, J.R., Koo, O.J., Sohn, I., Lee, W.Y., Kim, H.C., Yun, S.H., Cho, Y.B., Choi, M.A., et al. (2022). PRRX1 is a master transcription factor of stromal fibroblasts for myofibroblastic lineage progression. Nat. Commun. *13*, 2793. https://doi.org/10.1038/s41467-022-30484-4.

2. Kang, H.J., Oh, J.H., Chun, S.M., Kim, D., Ryu, Y.M., Hwang, H.S., Kim, S.Y., An, J., Cho, E.J., Lee, H., et al. (2019). Immunogenomic landscape of hepatocellular carcinoma with immune cell stroma and EBV-positive tumor-infiltrating lymphocytes. J. Hepatol. *71*, 91–103. https://doi.org/10.1016/j.jhep.2019.03.018.

3. André, T., Shiu, K.K., Kim, T.W., Jensen, B.V., Jensen, L.H., Punt, C., Smith, D., Garcia-Carbonero, R., Benavides, M., Gibbs, P., et al. (2020). Pembrolizumab in microsatellite-instability-high advanced colorectal cancer. N. Engl. J. Med. *383*, 2207–2218. https://doi.org/10.1056/NEJMoa2017699.

4. Cho, E.J., Kim, M., Jo, D., Kim, J., Oh, J.H., Chung, H.C., Lee, S.H., Kim, D., Chun, S.M., Kim, J., et al. (2021). Immuno-genomic classification of colorectal cancer organoids reveals cancer cells with intrinsic immunogenic properties associated with patient survival. J. Exp. Clin. Cancer Res. *40*, 230. https://doi.org/10.1186/s13046-021-02034-1.

5. Young, L.S., Yap, L.F., and Murray, P.G. (2016). Epstein-Barr virus: more than 50 years old and still providing surprises. Nat. Rev. Cancer *16*, 789–802. https://doi.org/10.1038/nrc.2016.92.

6. Callan, M.F.C. (2004). The immune response to Epstein-Barr virus. Microb. Infect. *6*, 937–945. https://doi.org/10.1016/j.micinf.2004.04.014.

7. Bortolomeazzi, M., Keddar, M.R., Montorsi, L., Acha-Sagredo, A., Benedetti, L., Temelkovski, D., Choi, S., Petrov, N., Todd, K., Wai, P., et al. (2021). Immunogenomics of colorectal cancer response to checkpoint blockade: analysis of the KEYNOTE 177 trial and validation cohorts. Gastroenterology *161*, 1179–1193. https://doi.org/10.1053/j.gastro.2021.06.064.

8. McNamara, M.G., Jacobs, T., Lamarca, A., Hubner, R.A., Valle, J.W., and Amir, E. (2020). Impact of high tumor mutational burden in solid tumors and challenges for biomarker application. Cancer Treat Rev. *89*, 102084. https://doi.org/10.1016/j.ctrv.2020.102084.

9. Smatti, M.K., Al-Sadeq, D.W., Ali, N.H., Pintus, G., Abou-Saleh, H., and Nasrallah, G.K. (2018). Epstein-barr virus epidemiology, serology, and genetic variability of LMP-1 oncogene among healthy population: an update. Front. Oncol. *8*, 211. https://doi.org/10.3389/fonc.2018.00211.

10. Weiskopf, D., Weinberger, B., and Grubeck-Loebenstein, B. (2009). The aging of the immune system. Transpl. Int. *22*, 1041–1050.

https://doi.org/10.1111/j.1432-2277.2009.00927.x.

11. Fujiwara, S., Imadome, K.I., and Takei, M. (2015). Modeling EBV infection and pathogenesis in new-generation humanized mice. Exp. Mol. Med. *47*, e135. https://doi.org/10.1038/emm.2014.88.

12. Münz, C. (2017). Humanized mouse models for Epstein Barr virus infection. Curr. Opin. Virol. *25*, 113–118. https://doi.org/10.1016/j.coviro.2017.07.026.

13. Newman, A.M., Liu, C.L., Green, M.R., Gentles, A.J., Feng, W., Xu, Y., Hoang, C.D., Diehn, M., and Alizadeh, A.A. (2015). Robust enumeration of cell subsets from tissue expression profiles. Nat. Methods *12*, 453–457. https://doi.org/10.1038/nmeth.3337.

14. Subramanian, A., Tamayo, P., Mootha, V.K., Mukherjee, S., Ebert, B.L., Gillette, M.A., Paulovich, A., Pomeroy, S.L., Golub, T.R., Lander, E.S., and Mesirov, J.P. (2005). Gene set enrichment analysis: a knowledge-based approach for interpreting genome-wide expression profiles. Proc. Natl. Acad. Sci. USA *102*, 15545–15550. https://doi.org/10.1073/pnas.0506580102.

15. Innis, S.E., Reinaltt, K., Civelek, M., and Anderson, W.D. (2021). GSEAplot: a package for customizing gene set enrichment analysis in R. J. Comput. Biol. *28*, 629–631. https://doi.org/10.1089/cmb.2020.0426.

16. Wu, T., Hu, E., Xu, S., Chen, M., Guo, P., Dai, Z., Feng, T., Zhou, L., Tang, W., Zhan, L., et al. (2021). clusterProfiler 4.0: a universal enrichment tool for interpreting omics data. Innovation *2*, 100141. https://doi.org/10.1016/j.xinn.2021.100141.

17. Hänzelmann, S., Castelo, R., and Guinney, J. (2013). GSVA: gene set variation analysis for microarray and RNA-seq data. BMC Bioinf. *14*, 7. https://doi.org/10.1186/1471-2105-14-7.

18. van der Leun, A.M., Thommen, D.S., and Schumacher, T.N. (2020). CD8(+) T cell states in human cancer: insights from single-cell analysis. Nat. Rev. Cancer *20*, 218–232. https://doi.org/10.1038/s41568-019-0235-4.

19. Chung, H.C., Cho, E.J., Lee, H., Kim, W.K., Oh, J.H., Kim, S.H., Lee, D., and Sung, C.O. (2021). Integrated single-cell RNA sequencing analyses suggest developmental paths of cancer-associated fibroblasts with gene expression dynamics. Clin. Transl. Med. *11*, e487. https://doi.org/10.1002/ctm2.487.

20. Elyada, E., Bolisetty, M., Laise, P., Flynn, W.F., Courtois, E.T., Burkhart, R.A., Teinor, J.A., Belleau, P., Biffi, G., Lucito, M.S., et al. (2019). Cross-species single-cell analysis of pancreatic ductal adenocarcinoma reveals antigen-presenting cancer-associated fibroblasts. Cancer Discov. *9*, 1102–1123. https://doi.org/10.1158/2159-8290.Cd-19-0094.

21. Ellrott, K., Bailey, M.H., Saksena, G., Covington, K.R., Kandoth, C., Stewart, C., Hess, J., Ma, S., Chiotti, K.E., McLellan, M., et al. (2018). Scalable open science approach for mutation calling of tumor exomes using multiple genomic pipelines. Cell Syst. *6*, 271–281.e7. https://doi.org/10.1016/j.cels.2018.03.002.

22. Mayakonda, A., Lin, D.C., Assenov, Y., Plass, C., and Koeffler, H.P. (2018). Maftools: efficient and comprehensive analysis of somatic variants in cancer. Genome Res. *28*, 1747–1756. https://doi.org/10.1101/gr.239244.118.

23. Chen, Y., Yao, H., Thompson, E.J., Tannir, N.M., Weinstein, J.N., and Su, X. (2013). VirusSeq: software to identify viruses and their integration sites using next-generation sequencing of human cancer tissue. Bioinformatics *29*, 266–267. https://doi.org/10.1093/bioinformatics/bts665.

24. Buchhalter, I., Rempel, E., Endris, V., Allgäuer, M., Neumann, O., Volckmar, A.L., Kirchner, M., Leichsenring, J., Lier, A., von Winterfeld, M., et al. (2019). Size matters: dissecting key parameters for panel-based tumor mutational burden analysis. Int. J. Cancer *144*, 848–858. https://doi.org/10.1002/ijc.31878.

25. Oh, J.H., Jang, S.J., Kim, J., Sohn, I., Lee, J.Y., Cho, E.J., Chun, S.M., and Sung, C.O. (2020). Spontaneous mutations in the single TTN gene represent high tumor mutation burden. NPJ Genom. Med. *5*, 33. https://doi.org/10.1038/s41525-019-0107-6.

STAR★METHODS

KEY RESOURCES TABLE

REAGENT or RESOURCE	SOURCE	IDENTIFIER
Biological samples		
Colorectal cancer tissues	Asan Medical Center	N/A
Deposited data		
Colorectal cancer bulk tissue RNA-seq	Cho et al.[4]	GSE171680
Colorectal cancer organoid RNA-seq	Cho et al.[4]	GSE171681
Oligonucleotides		
EBER1 and EBER2	Ventana	Cat# 800–2842
Software and algorithms		
CIBERSORT	Newman et al.[13]	https://cibersortx.stanford.edu/
Gene Set Enrichment Analysis (GSEA v4.0.2)	Subramanian et al.[14]	https://www.gsea-msigdb.org/gsea/index.jsp
Gene Set Variation Analysis (GSVA v1.38.2)	Hänzelmann et al.[17]	https://bioconductor.org/packages/release/bioc/html/GSVA.html
ClusterProfiler (v4.4.4)	Wu et al.[16]	https://bioconductor.org/packages/release/bioc/html/clusterProfiler.html
Maftools (v2.6.5)	Mayakonda et al.[22]	https://www.bioconductor.org/packages/devel/bioc/vignettes/maftools/inst/doc/maftools.html
VirusSeq	Chen et al.[23]	https://odin.mdacc.tmc.edu/~xsu1/VirusSeq.html
R	N/A	https://cran.r-project.org/

RESOURCE AVAILABILITY

Lead contact

Further information and requests for resources should be directed to and will be fulfilled by the lead contact, Chang Ohk Sung (co.sung@amc.seoul.kr)

Materials availability

This study did not generate new unique reagents.

Data and code availability

- RNA-seq data have been deposited at Gene Expression Omnibus (https://www.ncbi.nlm.nih.gov/geo/) and are publicly available. Accession numbers are listed in the key resources table(GEO: GSE171680 and GEO: GSE171681).
- This paper dose not report original code.
- Any additional information required to reanalyze the data reported in this paper is available from the lead contact upon request.

EXPERIMENTAL MODEL AND SUBJECT DETAILS

Clinical samples and data

A total of 87 patients (51 males and 36 females) with CRC were included, who were part of the same cohort from our previous study for CRC organoid model construction.[4] The mean age at diagnosis was 62.5 years (range from 28 to 94 years). The detailed clinical information for this cohort has been published previously.[4] Briefly, The normalized gene expression profiles from RNA sequencing (RNA-seq) for CRC organoid and

matched primary cancer tissue, which has been deposited at Gene Expression Omnibus (GEO; https://www.ncbi.nlm.nih.gov/geo; accession no. GSE171682) from our previous study,[4] were also used for this study. Raw RNA-seq data (fastq file) and MAF (mutation annotation file) data from targeted DNA sequencing for both cancer organoids and primary cancer tissues of the 87 patients with CRC were obtained from our previous study.[4] This study was approved by the Ethics Committee of Asan Medical Center, Seoul, Korea (IRB no. 2020–0214).

METHOD DETAILS

EBV-encoded RNA-in situ hybridization

EBV-encoded RNA-in situ hybridization (EBER-ISH) was performed using a Bench Mark XT autostainer (Ventana Medical Systems, Tucson, AZ, USA) with a Ventana ISH iVIEW Blue Detection Kit (Catalog no. 800–092) and INFORM EBER probe (Catalog no. 800–2842, Ventana) in one representative whole slide section for each formalin-fixed & paraffin-embedded (FFPE) CRC tissue sample. The density of EBV-positive tumor infiltrating lymphocytes (TILs) was measured as the highest number of EBV-positive TILs per high power field (EBV/HPF) under the microscope by two pathologists (HJP & COS).

RNA-seq data analysis

The normalized gene expression profiles of the 87 CRC organoids and matched primary cancer tissues downloaded from GEO (accession no. GSE171682) were used for immune cell profiling and pathway analyses. From the RNA expression data of primary cancer tissue, profiling of tumor-infiltrating immune cells was performed using CIBERSORT with LM22 (22 immune cell types) gene signatures.[13] The sum of the scores for the 22 immune cell types in each sample was used as the total immune score.[2] Gene Set Enrichment Analysis (GSEA v4.0.2)[14] was used to identify cancer signaling pathways based on gene expression profiles in the primary cancer tissues or cancer cell organoids. GSEA plot was generated using the GSEAplot R package.[15] Gene ontology enrichment analysis and network analysis were performed using the ClusterProfiler v.4.0 R package.[16] Gene Set Variation Analysis (GSVA)[17] was used to score the activation of pathway gene sets for every sample. GSVA was also used to calculate the CD8 T cell exhaustion score using known genes (*LAG3*, *PDCD1*, *HAVCR2*, and *TIGIT*) for CD8 T cell exhaustion.[18] Myofibroblastic cancer-associated fibroblast (myCAF) and inflammatory CAF (iCAF) scores were calculated using myCAF and iCAF signature gene set,[19,20] respectively, using GSVA.

TCGA data

Raw RNA sequencing data (fastq file) for CRC were downloaded from dbGAP (approval No. #7043) in March 2022. For somatic mutation, TCGA MC3 MAF v3 (mc3.v0.2.8.PpUBLICmaf)[21] mutation profile data were downloaded. Upper-quartile normalized gene expression data, including 20,502 gene expression levels from the RNA-seq for CRC, were downloaded from Broad GDAC Firehose ((https://gdac.broadinstitute.org/). The gene expression level was further transformed by log2(expression value +1). The corresponding clinical data were obtained from the TCGA cBioPortal (https://www.cbioportal.org/).

Mutationdata analysis

MAF format data, including somatic mutation profiles from the TCGA and AMC cohorts, were used to identify different somatic mutations between EBV-positive and EBV-negative tumors. Visualization of somatic mutations was performed using Maftools R package.[22]

Detection of EBV in RAN-seq data

VirusSeq[23] was used for EBV read discovery from paired-end RNA-seq fastq files. After aligning reads against human genome reference (version hg19), the unmapped non-human sequences generated by subtracting the human sequences re-aligned against all known viral sequences, including EBV genome from VirusSeq source site (https://odin.mdacc.tmc.edu/~xsu1/VirusSeq.html). EBV reference genome included Humanherpesvirus4completewildtypeg_AJ507799, strainAG876_DQ279927, and strainGD1_AY961628).

Estimation of tumor mutation burden (TMB)

All SNV and InDel types, including synonymous and non-synonymous mutations in all exon regions and splice sites, were used to calculate TMB.[24,25] This method was applied to the TCGA mutation profile from the whole exome sequencing of CRC.

Statistics

Wilcoxon rank-sum test or Kruskal-Wallis test was performed to compare the differences in continuous variables. Correlation analysis was performed using Spearman's correlation analysis. Fisher's exact test was used to evaluate the differences between categorical variables. Log-rank test was performed to evaluate survival differences between groups. Multivariate Cox proportional hazards regression and logistic regression analyses were also performed. All statistical analyses were performed using R version 4.2.0.